Received: 27 December 2022 | Revised: 27 February 2023 | Accepted: 1 March 2023

DOI: 10.1097/HEP.0000000000000375

ORIGINAL ARTICLE

Membrane phospholipid remodeling modulates nonalcoholic steatohepatitis progression by regulating mitochondrial homeostasis

Ye Tian[1] | Matthew J. Jellinek[2] | Kritika Mehta[3] | Sun Mi Seok[4] | Shanny H. Kuo[5] | Wei Lu[1] | Ruicheng Shi[1] | Richard Lee[6] | Gee W. Lau[5] | Jongsook Kim Kemper[4,7] | Kai Zhang[3] | David A. Ford[2] | Bo Wang[1,7,8]

[1]Department of Comparative Biosciences, College of Veterinary Medicine, University of Illinois at Urbana-Champaign, Urbana, Illinois, USA

[2]Department of Biochemistry and Molecular Biology, Center for Cardiovascular Research, Saint Louis University, St. Louis, Missouri, USA

[3]Department of Biochemistry, School of Molecular and Cellular Biology, University of Illinois at Urbana-Champaign, Urbana, Illinois, USA

[4]Department of Molecular and Integrative Physiology, School of Molecular and Cellular Biology, University of Illinois at Urbana-Champaign, Urbana, Illinois, USA

[5]Department of Pathobiology, College of Veterinary Medicine, University of Illinois at Urbana-Champaign, Urbana, Illinois, USA

[6]Ionis Pharmaceuticals, Carlsbad, California, USA

[7]Cancer Center at Illinois, University of Illinois at Urbana-Champaign, Urbana, Illinois, USA

[8]Division of Nutritional Sciences, College of Agricultural, Consumer and Environmental Sciences, University of Illinois at Urbana-Champaign, Urbana, Illinois, USA

Correspondence
Bo Wang, 3840 VMBSB, 2001 S Lincoln Ave., Urbana, IL 61802, USA.
Email: bowang@illinois.edu

Abstract

Background and Aims: NASH, characterized by inflammation and fibrosis, is emerging as a leading etiology of HCC. Lipidomics analyses in the liver have shown that the levels of polyunsaturated phosphatidylcholine (PC) are decreased in patients with NASH, but the roles of membrane PC composition in the pathogenesis of NASH have not been investigated. Lysophosphatidylcholine acyltransferase 3 (LPCAT3), a phospholipid (PL) remodeling enzyme that produces polyunsaturated PLs, is a major determinant of membrane PC content in the liver.

Approach and Results: The expression of *LPCAT3* and the correlation between its expression and NASH severity were analyzed in human patient samples. We examined the effect of *Lpcat3* deficiency on NASH progression using *Lpcat3* liver-specific knockout (LKO) mice. RNA sequencing, lipidomics, and metabolomics were performed in liver samples. Primary hepatocytes and hepatic cell lines were used for *in vitro* analyses. We showed that *LPCAT3* was dramatically suppressed in human NASH livers, and its expression was inversely correlated with NAFLD activity score and fibrosis stage. Loss of *Lpcat3* in mouse liver promotes both spontaneous and diet-induced NASH/HCC. Mechanistically, *Lpcat3* deficiency enhances reactive oxygen species production due to impaired mitochondrial homeostasis. Loss of *Lpcat3* increases inner mitochondrial membrane PL saturation and elevates stress-induced autophagy, resulting in reduced mitochondrial content

Abbreviations: CL, cardiolipin; EM, electron microscopy; FAO, fatty acid oxidation; FFA, free fatty acids; GO, gene ontology; 4-HNE, 4-hydroxynonenal; GSH, glutathione; GWAS, genome-wide association studies; H&E, hematoxylin and eosin; IMM, inner mitochondrial membrane; JNK, c-Jun-N-terminal kinase; LKO, Lpcat3 liver knockout mice; LPCAT3, lysophosphatidylcholine acyltransferase 3; MARC1, mitochondrial amidoxime reducing component 1; mtDNA, mitochondrial DNA; NAS, NAFLD activity score; NEFA, nonesterified fatty acid; OCR, oxygen consumption rate; OxPhos, oxidative phosphorylation; PC, phosphatidylcholine; PE, phosphatidylethanolamine; PEMT, phosphatidylethanolamine N-methyltransferase; PGE2, prostaglandin E2; PL, phospholipid; PLA2s, phospholipase A2s; PNPLA3, patatin-like phospholipase domain-containing 3; ROS, reactive oxygen species; TG, triglyceride; TMSF62, transmembrane 6 superfamily member 2 α-SMA, α-smooth muscle actin.

Supplemental Digital Content is available for this article. Direct URL citations are provided in the HTML and PDF versions of this article on the journal's website, www.hepjournal.com.

and increased fragmentation. Furthermore, overexpression of *Lpcat3* in the liver ameliorates inflammation and fibrosis of NASH.

Conclusions: These results demonstrate that membrane PL composition modulates the progression of NASH and that manipulating LPCAT3 expression could be an effective therapeutic for NASH.

INTRODUCTION

NAFLD has become the most common chronic liver disease around the world, affecting ~25% of the adults.[1] With complex yet poorly understood pathologies, liver can progress from simple steatosis to NASH, featured with inflammation and fibrosis, and finally to cirrhosis and HCC.[2] Genome-wide association studies (GWAS) have identified single nucleotide polymorphism in several genes to be closely associated with the risk or severity of NASH development, including patatin-like phospholipase domain-containing 3 (*PNPLA3*), transmembrane 6 superfamily member 2 (*TMSF62*), and mitochondrial amidoxime reducing component 1 (*MARC1*).[3,4] However, the mechanisms underlying these genetic variants in the pathogenesis of NASH are not clear.

Lipidomics analyses in the liver have shown that the levels of polyunsaturated phosphatidylcholine (PC), especially arachidonic acid (20:4)-containing PC, are decreased in NASH, while total PC content is not altered.[5,6] Interestingly, recent studies have demonstrated that hepatic polyunsaturated PC levels are correlated with NASH-related genetic variants. For example, the levels of polyunsaturated PC species are increased in the liver of patients carrying a protective variant in *MARC1* gene.[7] In contrast, patients with NASH-promoting variants in *TM6SF2* and *PNPLA3* genes have reduced polyunsaturated PCs and increased saturated PCs in the liver compared with noncarriers.[8,9] These studies suggest that hepatic polyunsaturated PC content is inversely correlated with the risk or severity of NASH in humans. However, the role of altered PC composition in the pathogenesis of NASH and the underlying mechanisms have not been investigated.

The composition of membrane PCs is regulated by Lands cycle, where PCs are remodeled by substitution of the fatty acyl chain on the sn-2 site through the sequential activity of phospholipase A2s (PLA2s) and lysophosphotidylcholine acyltransferases (LPCATs).[10] LPCAT3 is the most abundant LPCAT in the livers of both human and mouse. Because of its substrate preference of polyunsaturated fatty acyl chains, LPCAT3 has been shown to be a critical determinant of membrane PC composition, especially the levels of polysaturated PCs.[11] Previous studies have shown that loss of *Lpcat3* in the liver selectively reduces membrane polyunsaturated PCs without affecting total PC levels, which results in increased membrane saturation, impaired VLDL secretion, and hepatic steatosis.[12] However, whether and how LPCAT3 modulates the progression of NAFLD from steatosis to NASH remain elusive.

In this study, we demonstrate that *LPCAT3* is suppressed in human NASH livers and its expression is inversely correlated with NAFLD activity score (NAS) and fibrosis stage. We show that deletion of *Lpcat3* in mouse liver leads to the development of spontaneous NASH and HCC with age. *Lpcat3* liver knockout (LKO) mice are also prone to diet-induced NASH and HCC progression. We further show that loss of *Lpcat3* reduces PC and cardiolipin unsaturation in the inner mitochondrial membrane (IMM) and exacerbates mitochondrial oxidation, which leads to the overproduction of reactive oxygen species (ROS). Moreover, *Lpcat3* deficiency decreases mitochondrial DNA content and induces fragmented mitochondrial morphology, likely due to enhanced mitochondrial damage and autophagy. Finally, we show that overexpression of *Lpcat3* in the liver ameliorates inflammation and fibrosis in a diet-induced mouse NASH model. These data provide strong evidence that changes in membrane PC composition *per se* are sufficient to drive the initiation and progression of NASH and that manipulating PC content through *LPCAT3* activation could be a novel therapeutic approach for NASH.

METHODS

Animal models

All animal procedures were conducted in compliance with protocols approved by the Institutional Animal Care and Use Committee at University of Illinois at Urbana-Champaign. *Lpcat3*$^{fl/fl}$ and *Lpcat3*$^{fl/fl}$, *Albumin-Cre* mice have been described.[12] Briefly, gene targeting vector was electroporated into JM8A1.N3 ES cell line from C57BL/6N mice. Targeted ES cell clones were injected into C57BL/6J blastocysts to generate chimeric mice, which were bred with C57BL/6J mice to obtain heterozygous knockout mice (*Lpcat3*$^{+/-}$). *Lpcat3*$^{+/-}$ mice were mated with mice expressing a Flpe recombinase transgene on C57BL/6J background to generate *Lpcat3*$^{Fl/+}$ mice, which were crossed with albumin-*Cre* on C57BL/6J background to generate *Lpcat3*$^{Fl/Fl}$, *Albumin-Cre*+(LKO) and *Lpcat3*$^{Fl/Fl}$, *Albumin-Cre*− (control) mice. Both LKO

and control mice were on mixed 87.5% C57BL/6J and 12.5% C57BL/6N background. All mice were housed under pathogen-free conditions in a temperature-controlled room with a 12-hour light/dark cycle. Mice were fed chow diet (Lab Diet #5001) or NASH diet (Envigo, TD.120528) with a high-sugar solution (23.1 g/L D-fructose and 18.9 g/L D-glucose). All experiments were performed with male mice. Mice were sacrificed after 6-hour fasting, and liver tissues were collected and snap frozen in liquid nitrogen and stored at −80 °C. Mouse blood was collected by retro-orbital bleeding before sacrificing or by tail bleeding, and serum was obtained by centrifugation.

NAFLD human patient study

The NAFLD human patient liver specimens were described.[13] Liver specimens from 15 unidentifiable normal individuals without known liver diseases, 15 individuals with steatosis, and 15 individuals with severe NASH-fibrosis were obtained from the Liver Tissue Cell Procurement and Distribution System that operates under a contract from the NIH. Because the specimens or data were not collected specifically for this study and we do not have access to the subject identifiers linked to the specimens or data, this study is not considered human subjects research and ethical approval was not required (see section 46.104 in Part 46–Protection of Human Subjects in the Electronic Code of Federal Regulations). The correlation between *LPCAT3* expression and NAS/fibrosis stage was analyzed from GSE193084.[14]

Phospholipid analysis

Phospholipids (PLs) were quantified as described.[15–17] Lipids were extracted from liver tissues and isolated IMM through modified Bligh-Dyer extraction with the addition of lipid class-specific internal standards as described.[18] Lipidomics were performed using a Q Exactive mass spectrometer paired with a Vanquish UHPLC System (Thermo Scientific).[19] Chromatographic separation was achieved using a Accucore C30 column 2.1 × 150 mm (Thermo Scientific) with mobile phase A composed of 60% acetonitrile, 40% water, 10 mM ammonium formate, and 0.1% formic acid and mobile phase B composed of 90% isopropanol, 10% acetonitrile with 2 mM ammonium formate, and 0.02% formic acid. CL, PC, and PE species were analyzed through parallel reaction monitoring and quantitated with the application of isotopomer corrections and normalization to the mass of mitochondrial protein for each sample. Aliphatic constituents were confirmed through analyzing the MS/MS spectra obtained for each species for corresponding fragments (eg, *m/z* 281.2 for C18:1).

Quantification and statistical analysis

All data are presented as mean ± SEM. Most of our data followed normal distribution, and comparisons were performed using the unpaired 2-tailed Student *t* test, with significance defined as a p-value <0.05. For data that do not follow normal distribution, nonparametric *t* test was used to calculate the p-value. GraphPad Prism 9.0 (San Diego, CA) was used for all statistical analysis. Western blot data were quantified using ImageJ.

Data availability

RNA sequencing data have been deposited at Gene Expression Omnibus (accession numbers GSE218075). Original data or any additional information required to reanalyze the data reported in this paper will be available from the lead contact on request (Supplemental Materials and Methods, http://links.lww.com/HEP/F16). Detailed materials and methods are available in the supplementary information.

RESULTS

Hepatic *LPCAT3* expression is inversely correlated with NAFLD progression

To investigate whether *LPCAT3* is dysregulated during the progression of NAFLD, we measured its mRNA levels in liver biopsies from a cohort of normal individuals, patients with NAFLD with simple steatossis, and patients with NASH with fibrosis. Real-time RT-PCR results showed that *LPCAT3* is gradually downregulated in steatosis and NASH livers (Figure 1A). Next, we analyzed *LPCAT3* expression in another published transcriptome data with histological gradings of liver biopsies obtained from 213 patients with NAFLD (GSE193084).[14] Association analysis showed that *LPCAT3* expression was inversely correlated with NAS and fibrosis stage (Figure 1B, C). These results demonstrate that downregulation of *LPCAT3* expression likely contributes to the progression of NAFLD and NASH.

Mice that lack *Lpcat3* in the liver develop spontaneous NASH and HCC with age

Next, we investigated if dysregulation of *LPCAT3* and PC composition are the driver or the consequence of NAFLD progression. We examined the livers of age-matched 16- to 24-month-old LKO mice on regular chow diet. The liver weight-to-body weight ratio was significantly increased in LKO mice (Figure 2A). Hepatic triglyceride (TG), nonesterified fatty acid (NEFA), and total and free cholesterol were significantly higher in LKO mice

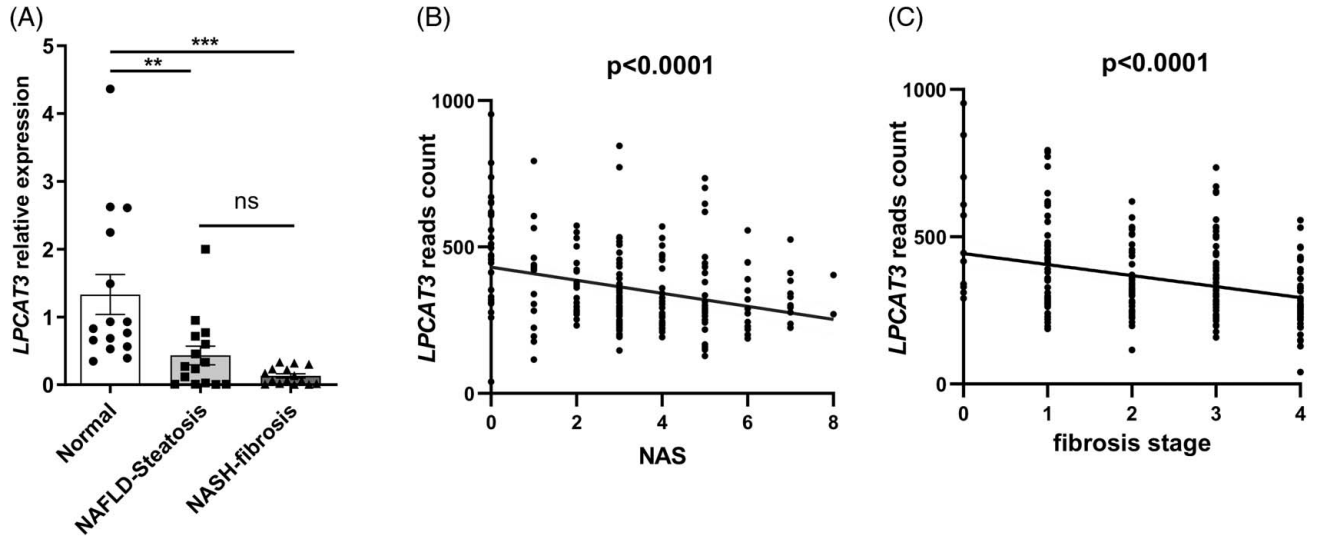

FIGURE 1 *LPCAT3* expression is reduced in patients with NASH, and liver-specific deletion of *Lpcat3* leads to NASH and HCC with age. (A) Hepatic expression of *LPCAT3* in human patients with NAFLD/NASH. Correlation between hepatic *LPCAT3* expression and NAS (B) and fibrosis stage (C) in human patients with NASH. Ninety-five percent confidence band of the best-fit line was shown by dashed curve. Data in (A) are presented as means ± SEM. Statistical analysis was performed with 1-way ANOVA (A) and linear regression (B and C). $^{**}p < 0.01$, $^{***}p < 0.001$. Abbreviation: NAS, NAFLD Activity Score.

(Figure 2B). Serum cholesterol and TG, but not NEFA, were decreased or trended toward a decrease in LKO mice (Supplemental Figure S1A–D, http://links.lww.com/HEP/F18). More strikingly, aged LKO mice exhibited histopathological manifestations of NASH in the absence of any dietary or chemical challenges. Histological analysis revealed moderate lipid accumulation in hepatocytes and massive central and intralobular infiltration of immune cells (Figure 2C). Signs of hepatocellular injury were also present in LKO livers as demonstrated by the presence of ballooning hepatocytes and Mallory-Denk bodies. Sirius red staining revealed increased fibrosis in LKO livers compared with controls (Figure 2C and D). Accordingly, LKO livers had a much higher NAS (Figure 2E). Strikingly, half (6 out of 12) of LKO mice developed spontaneous HCC, which was confirmed by positive staining of AFP (Figure 2F). These data strongly indicate that membrane PC composition is critical for liver homeostasis and that changes in PC composition caused by *Lpcat3* deficiency *per se* are sufficient to drive the pathogenesis of NASH and HCC.

Loss of *Lpcat3* promotes diet-induced NASH and HCC

Next, we tested whether loss of *Lpcat3* promotes diet-induced NASH development. We fed control and LKO mice a NASH-inducing diet (NASH diet), which has been shown to induce NASH in mouse liver that closely recapitulates human NASH.[20] LKO mice exhibited significantly higher liver weight-to-body weight ratio after 12 and 30 weeks of diet feeding (Supplemental Figure S2A, http://links.lww.com/HEP/F18). Lipid measurement showed higher hepatic TG and cholesterol levels in LKO livers (Supplemental Figure S2B, http://links.lww.com/HEP/F18), whereas hepatic NEFA and serum lipids were largely unchanged after 12 weeks of diet feeding (Supplemental Figure S2B, C, http://links.lww.com/HEP/F18). Histological analysis demonstrated that LKO mice developed more pronounced steatosis, lobular inflammation, and fibrosis compared with control mice as shown by hematoxylin and eosin and sirius red staining as early as 12 weeks on NASH diet (Figure 3A, B). Increased fibrosis was also confirmed by higher hydroxyproline levels in LKO livers (Supplemental Figure S2D, http://links.lww.com/HEP/F18). Immunostaining of α-smooth muscle actin, a marker of activated HSCs that is critical in liver fibrogenesis, manifested more activated HSCs in LKO livers (Figure 3A). Consequently, LKO mice showed much higher NAS after 12 weeks of diet feeding and trended toward an increase in 30-week fed livers (Figure 3C). In agreement with histology data, mRNA levels of TNF-alpha (*Tnfα*) and collagen synthesis genes were significantly upregulated in the liver of LKO mice (Figure 3D, E). Apoptotic cell death was significantly increased in LKO mice under NASH diet (Supplemental Figure S2E, http://links.lww.com/HEP/F18). Moreover, serum aspartate transaminase and alanine transaminase activities were also higher in LKO mice, indicating increased liver damages (Supplemental Figure S2F, http://links.lww.com/HEP/F18). As a result of more severe NASH, all LKO mice (7 out of 7) developed AFP-positive HCC after 50 weeks of diet feeding (Figure 3F). In contrast, only one-third (2 out of 6) of control mice had tumors. Moreover, LKO mice developed more tumors compared with control mice (Figure 3F).

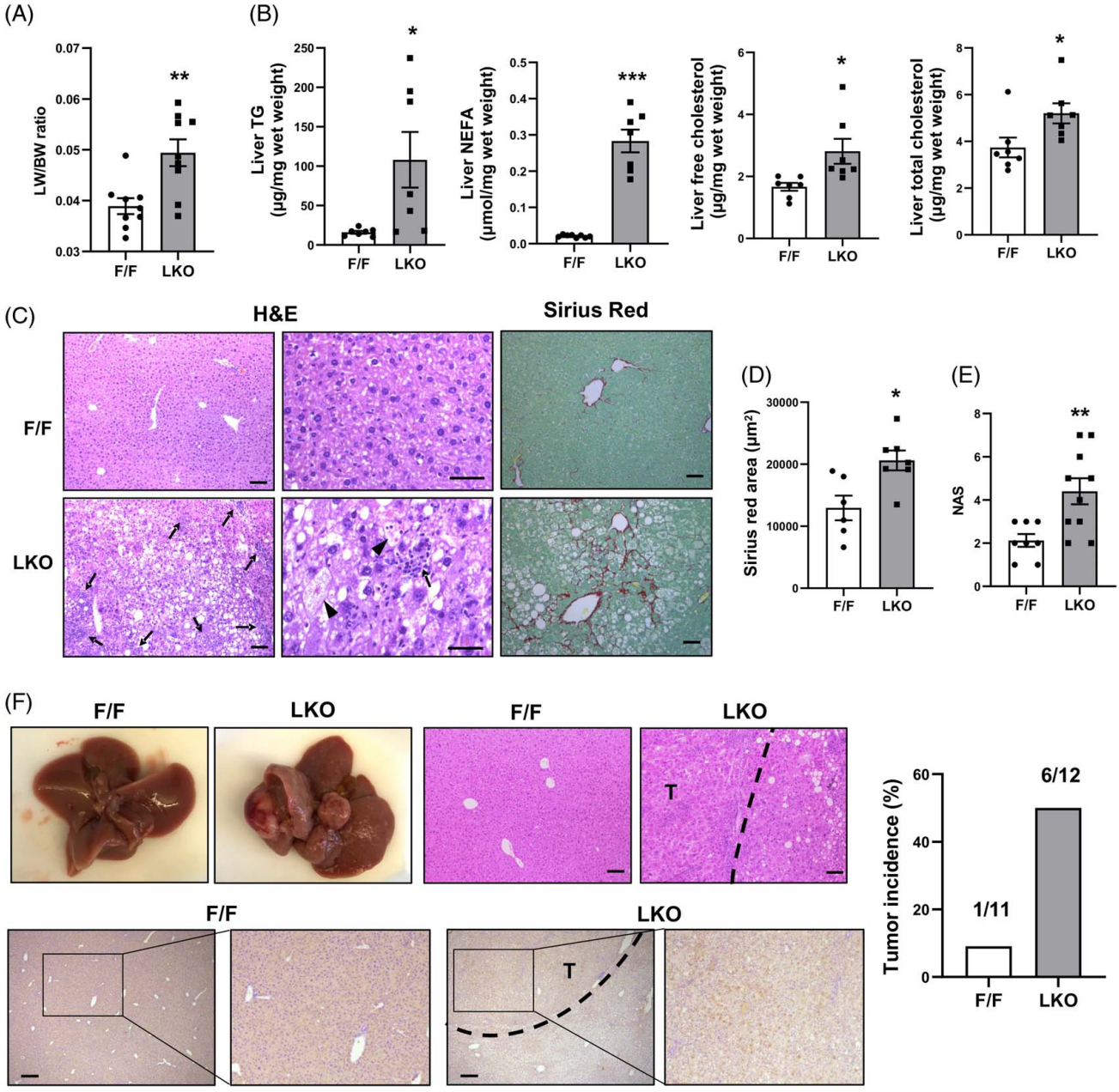

FIGURE 2 *Lpcat3* LKO mice develop spontaneous NASH and HCC with age. (A) LW to body weight (BW) ratio of 16- to 24-month-old control *Lpcat3*$^{fl/fl}$ (F/F) and *Lpcat3*$^{fl/fl}$ *Albumin-Cre* (LKO) mice on chow diet. (B) Hepatic triglyceride (TG), nonesterified fatty acid (NEFA), and free and total cholesterol levels in 16-24-month-old F/F and LKO mice on chow diet. (C) Hematoxylin and eosin (H&E) and Sirius Red staining of liver sections from 16-24-month-old F/F and LKO mice on chow diet (scale bar, 100 μm). Arrows denote immune cell infiltration, and arrowheads show ballooning hepatocytes. (D-E) Quantification of Sirius Red area (D) and NAS (E) for 16-24-month-old F/F and LKO mice on chow diet. (F) Liver images, H&E, AFP IHC staining, and tumor incidence of 16-24-month-old F/F and LKO mice on chow diet (T: tumor. scale bar, 100 μm). Data are presented as means ± SEM. Statistical analysis was performed with student's t test. *$p < 0.05$, **$p < 0.01$, ***$p < 0.001$. Abbreviations: BW, body weight; H&E, hematoxylin and eosin; LKO, *Lpcat3* liver-specific knockout; LW, Liver weight; NEFA, nonesterified fatty acid; TG, triglyceride.

Lpcat3 deficiency increases ROS production

Next, we sought to explore the mechanisms by which loss of *Lpcat3* promotes NASH progression. Previous studies have shown that acute knockdown of *Lpcat3* in the liver induces ER stress,[21] which is known to promote cell death and NASH progression.[22] Real-time RT-PCR analysis showed that most of the ER stress genes, except *Atf3*, were not altered in LKO livers after 12 weeks of diet feeding (Supplemental Figure S3A, http://links.lww.com/HEP/F18), suggesting that ER stress is unlikely a major contributor to NASH development in LKO mice. Next, we profiled gene expression in the livers of control and LKO mice fed NASH diet for 12 weeks by RNA sequencing analysis and found ~500

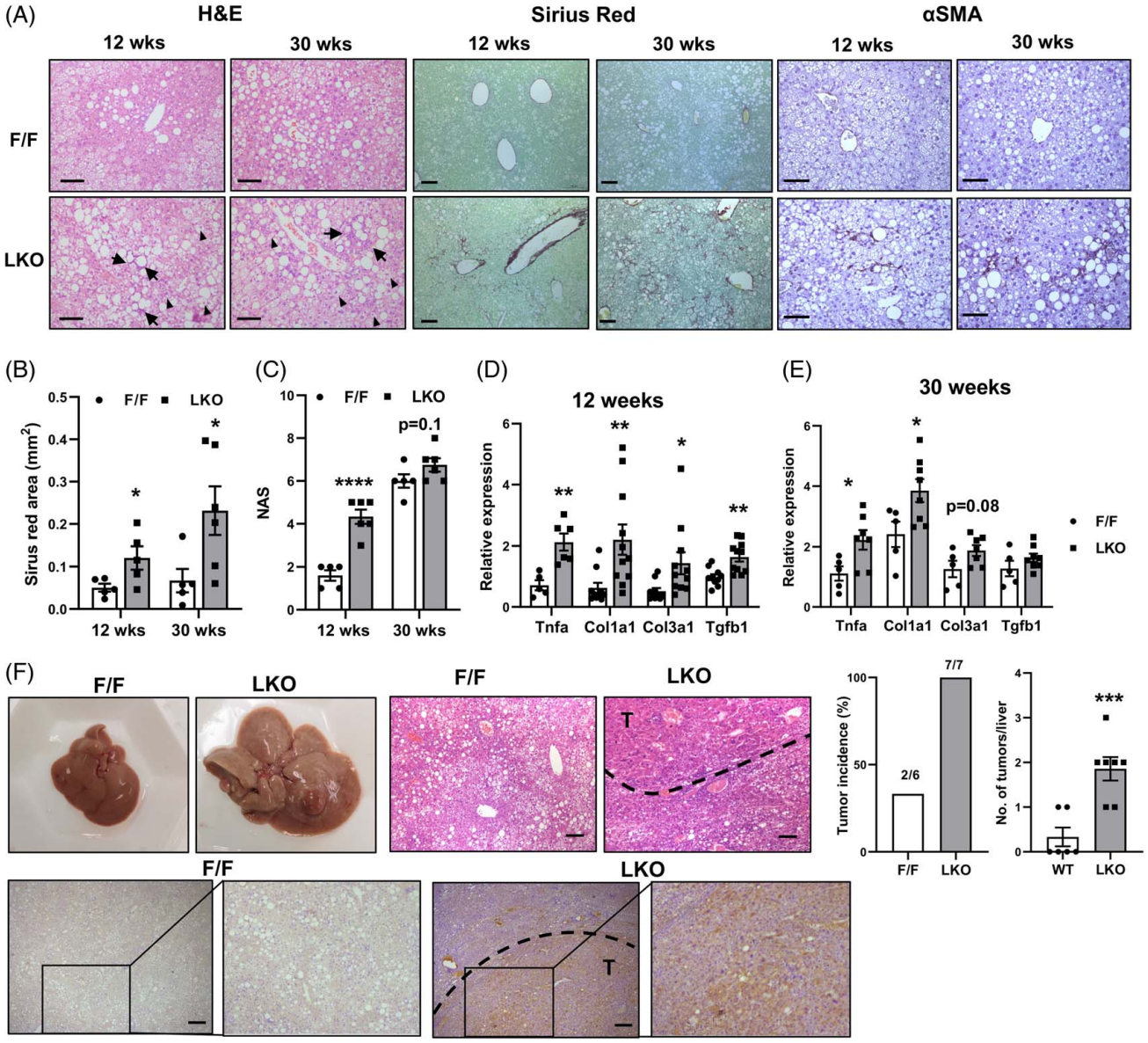

FIGURE 3 Loss of *Lpcat3* in the liver promotes diet-induced NASH and HCC. (A) H&E, Sirius Red, and immunohistochemistry of α-SMA of livers from F/F and LKO mice fed NASH diet for 12 and 30 weeks. Arrows denote immune cell infiltration, and arrowheads show ballooning hepatocytes (scale bar, 100 μm). Quantification of liver Sirius Red area (B) and NAS (C) of F/F and LKO mice fed NASH diet for 12 and 30 weeks. Hepatic mRNA levels of *Tnfα* and genes involved in fibrosis in F/F and LKO mice fed NASH diet for 12 (D) and 30 weeks (E). (F) Liver images, H&E, AFP staining, tumor incidence, and number of tumors per liver of F/F and LKO mice fed NASH diet for 54 weeks (T, tumor. scale bar, 100 μm). Data are presented as means ± SEM. Statistical analysis was performed with Student *t* test or multiple *t* test. *$p < 0.05$, **$p < 0.01$, ***$p < 0.001$, ****$p < 0.0001$. Abbreviations: α-SMA, α-smooth muscle actin; H&E, hematoxylin and eosin; LKO, *Lpcat3* liver-specific knockout.

upregulated genes and ~200 downregulated genes in LKO livers compared with controls (Supplemental Figure S3B, http://links.lww.com/HEP/F18). Among the upregulated genes, Gene Ontology (GO) analysis revealed strong enrichment for genes involved in inflammatory response and proinflammatory cytokines production in LKO livers (Figure 4A), which is consistent with enhanced inflammation in histology. Furthermore, ROS production was one of the upregulated GO terms in LKO livers. Interestingly, electron transport and proton transport were among the top downregulated GO terms in LKO livers (Figure 4B). Mitochondrial electron transport chain is a major site of ROS production.[23] Indeed, hepatic ROS levels were ~1.5-fold higher in LKO mice compared with controls (Figure 4C). Consistently, the levels of dehydroascorbic acid, a marker of oxidative stress,[24] were significantly increased in LKO livers (Supplemental Figure S3C, http://links.lww.com/HEP/F18). MitoSox staining of primary hepatocytes isolated from 9-week NASH diet-fed control and LKO mice further confirmed elevated ROS in the absence of *Lpcat3* (Supplemental Figure S3D, http://links.lww.com/HEP/F18 and 4D). Similar results were also observed in *Lpcat3* acute knockdown Hepa cells

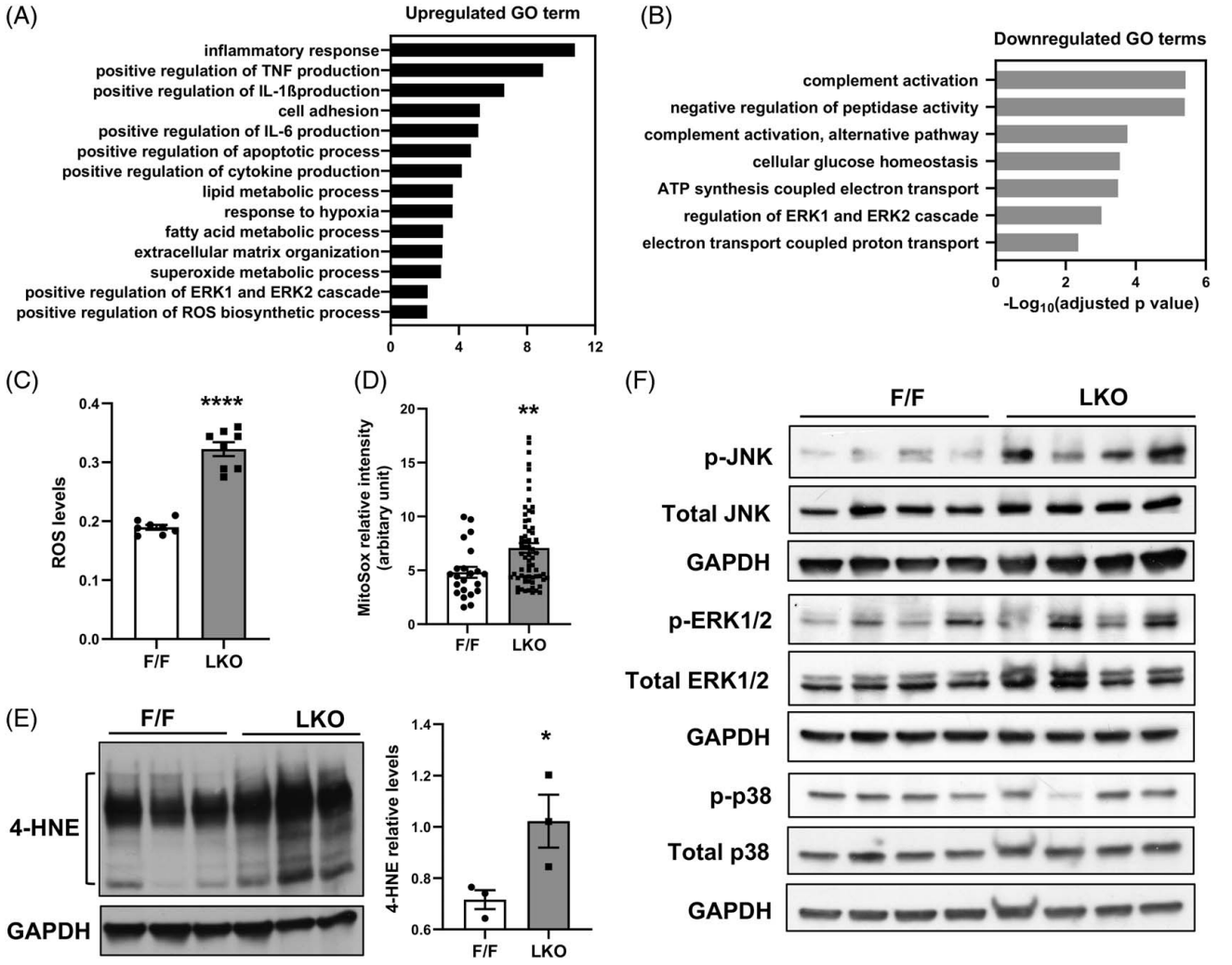

FIGURE 4 *Lpcat3* deficiency in the liver induces ROS production and causes oxidative stress. Enriched terms from GO analysis of significantly upregulated (A) and downregulated genes (B) in 12-week NASH diet-fed LKO livers compared to control F/F. (C) Total ROS levels in primary hepatocytes isolated from F/F and LKO mice fed with NASH diet for 9 weeks. (D) Quantification of mitosox staining in primary hepatocytes isolated from F/F and LKO mice fed with NASH diet for 9 weeks. (E) Immunoblot and quantification of 4-hydroxynonenal (4-HNE) in livers of F/F and LKO mice fed NASH diet for 12 weeks. (F) Immunoblot of MAPK pathways in livers of F/F and LKO mice fed NASH diet for 12 weeks. Data are presented as means ± SEM. Statistical analysis was performed with student's t test. *$p < 0.05$, **$p < 0.01$, ****$p < 0.0001$. Abbreviations: 4-HNE, 4-hydroxynonenal; GO, Gene Ontology; JNK, c-Jun-N-terminal kinase; LKO, Lpcat3 liver knockout mice.

(Supplemental Figure S3E,F, http://links.lww.com/HEP/F18). ROS is known to oxidize vital cellular components such as DNA, lipids, and proteins, thereby inducing cell death and liver damage.[25] The levels of 4-hydroxynonenal (4-HNE), a product of lipid peroxidation by ROS, was dramatically increased in LKO livers (Figure 4E). Previous studies have shown that oxidative stress and lipid peroxidation activate c-Jun-N-terminal kinase (JNK) pathway in NASH livers.[26] Western blot analysis showed that JNK pathway was dramatically increased in LKO livers compared with controls, whereas 2 other MAPK pathways, ERK and p38 pathway, were not significantly altered (Figure 4F). Hepatocytes have developed a range of antioxidant strategies to cope with oxidative stress, including glutathione (GSH) and catalase in the peroxisome.[27] Measurement of GSH and GSH/GSSG ratio showed a trend toward an increase in LKO livers likely due to compensatory responses (Supplemental Figure S3G–H, http://links.lww.com/HEP/F18). In contrast, catalase levels were slightly reduced, albeit an increase in peroxisomal marker PMP70 (Supplemental Figure S3I, http://links.lww.com/HEP/F18). Nevertheless, these data demonstrated that loss of *Lpcat3* enhances ROS production, which likely contributes to the pathogenesis of NASH.

Lpcat3 deficiency impairs mitochondrial homeostasis

Mitochondria dysfunction plays a key role in the pathogenesis of NASH.[28] Further analysis of RNA sequencing

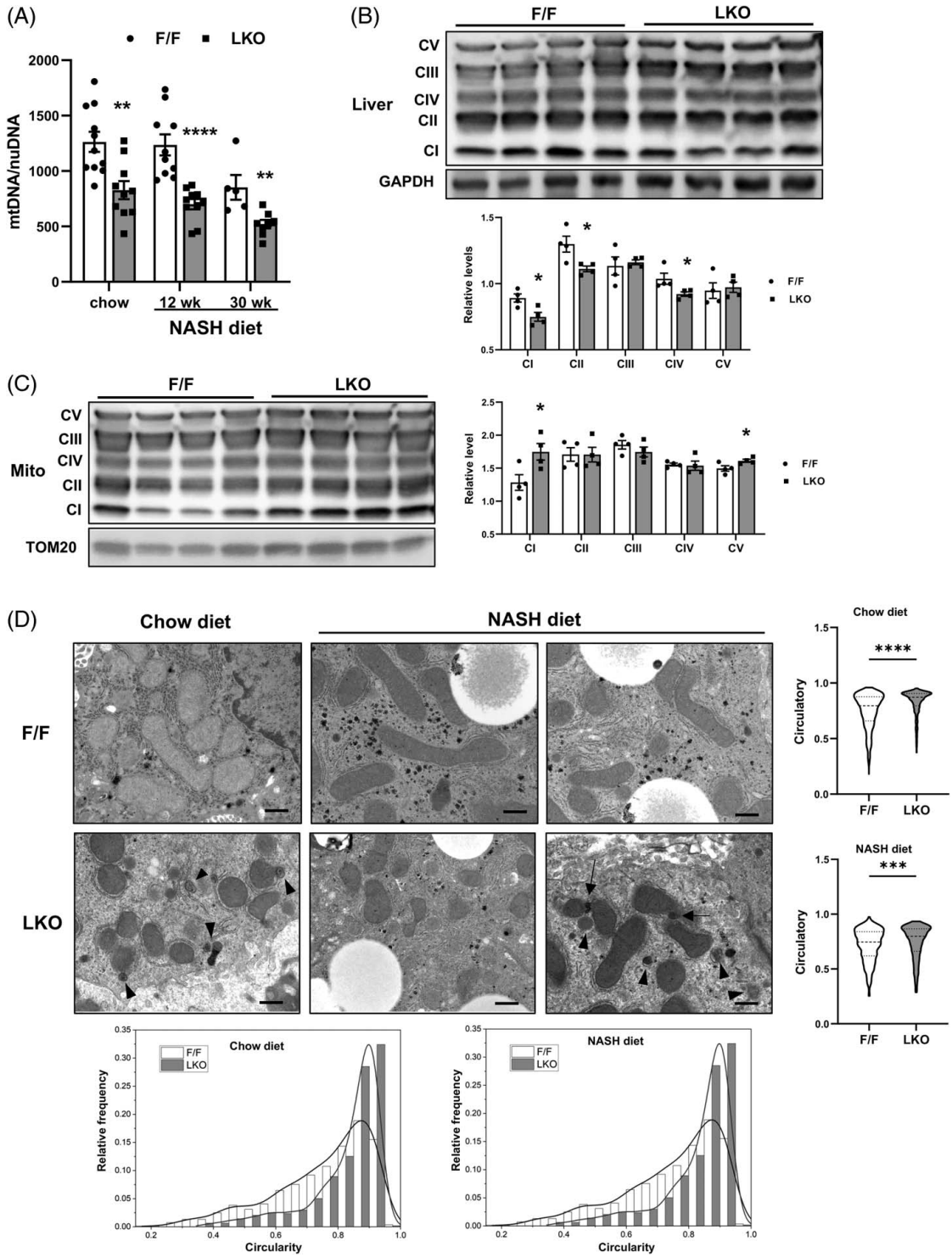

FIGURE 5 Deletion of *Lpcat3* in the liver impairs mitochondria homeostasis. (A) Mitochondrial DNA (mtDNA) content normalized to nuclear DNA (nuDNA) in livers of F/F and LKO mice on chow diet or NASH diet. Immunoblots and quantifications of oxidative phosphorylation (OxPhos) complexes in livers (B) or isolated mitochondria (C) from F/F and LKO mice fed NASH diet for 12 weeks. (D) Transmission electron microscopy (TEM) images of liver sections and distribution of hepatic mitochondrial circularity from chow diet or 12-week NASH diet-fed mice. Arrows show mitochondria undergoing fission and arrowheads show autophagosome-like structures (scale bar, 600 nm). Data in (A–C) are presented as means ± SEM. Data in (D) show median and quantiles. Statistical analysis was performed with multiple *t* test (A–C) and Kolmogorov-Smirnov test (D). The distribution curve in (D) was fit by Kernel Smooth. *$p < 0.05$, **$p < 0.01$, ***$p < 0.001$, ****$p < 0.0001$. Abbreviations: LKO, Lpcat3 liver knockout mice.

data showed that a majority of mitochondria-encoded genes were significantly downregulated in LKO livers (Supplemental Figure S4A, http://links.lww.com/HEP/F18). Strikingly, mitochondrial DNA (mtDNA) content was dramatically reduced in the livers of 3-month-old chow diet-fed and NASH diet-fed LKO mice (Figure 5A).

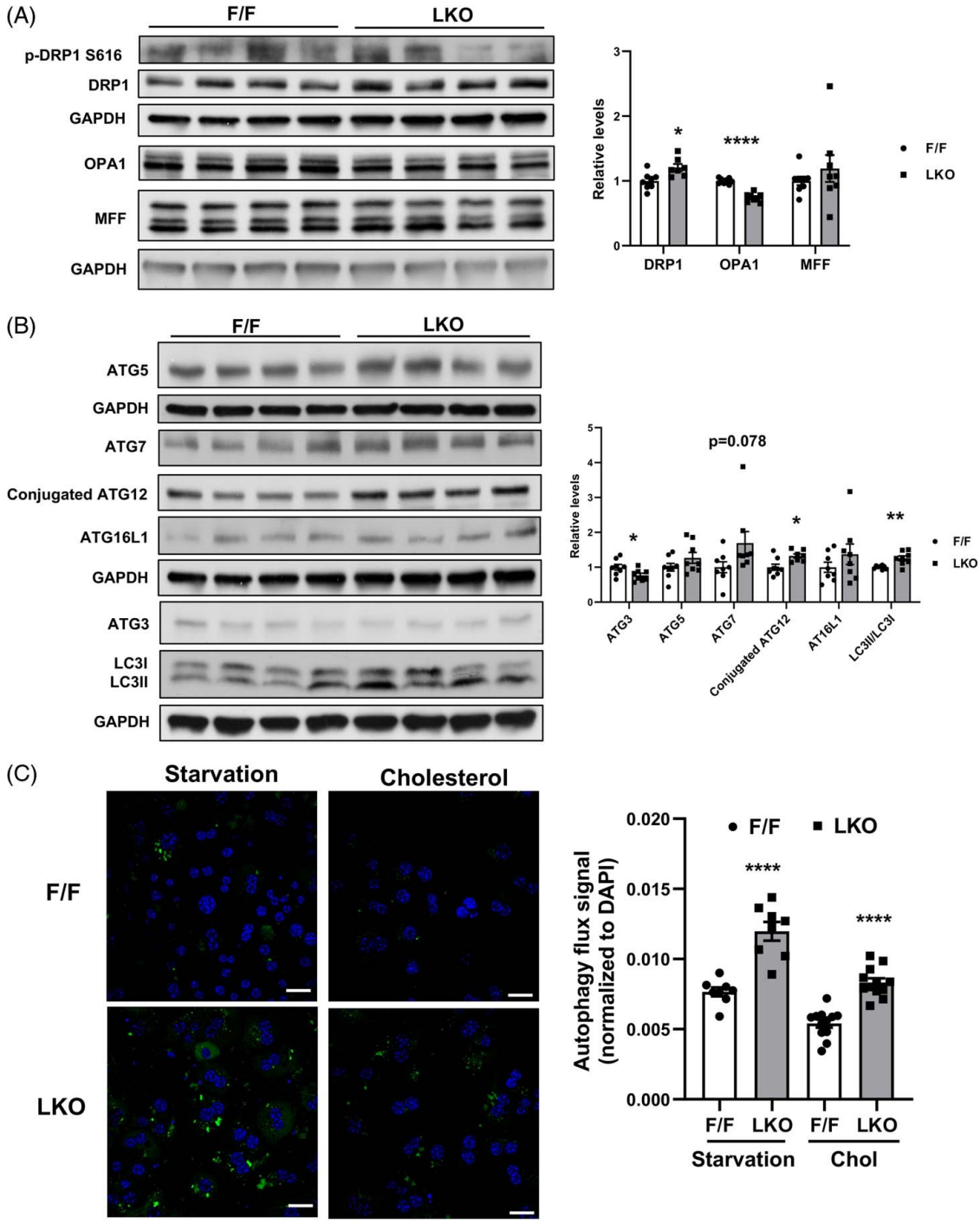

FIGURE 6 Loss of *Lpcat3* in the liver alters mitochondrial dynamics and promotes stress-induced autophagy. Representative immunoblots and quantifications of proteins involved in mitochondrial fusion and fission (A) and autophagy (B) in livers of F/F and LKO mice fed with NASH diet for 12 weeks. (C) Representative images and fluorescence signal readings of autophagic vacuoles staining in primary hepatocytes cultured in serum free medium or treated with cholesterol overnight. Data are presented as mean ± SEM. Statistical analysis was performed with Student *t* test. *$p < 0.05$, **$p < 0.01$, ***$p < 0.001$, ****$p < 0.0001$. Abbreviations: LKO, Lpcat3 liver knockout mice.

Furthermore, mtDNA content was gradually decreased with the progression of NAFLD in both control and LKO mice, suggesting that decrease in mitochondria content may contribute to disease progression. Consistent with reduced mitochondrial content in LKO livers, western blot analysis showed less mitochondrial respiratory complexes I, II, and IV in whole liver lysate (Figure 5B). Similarly, COX IV and TOM20, 2 mitochondrial proteins, were also reduced in LKO livers (Supplemental Figure S4B, http://links.lww.com/HEP/F18). In contrast, mitochondrial complexes I and V were increased in isolated mitochondria from LKO livers compared with controls (Figure 5C), probably as a compensation for the reduced mitochondrial content. The purity of isolated mitochondria

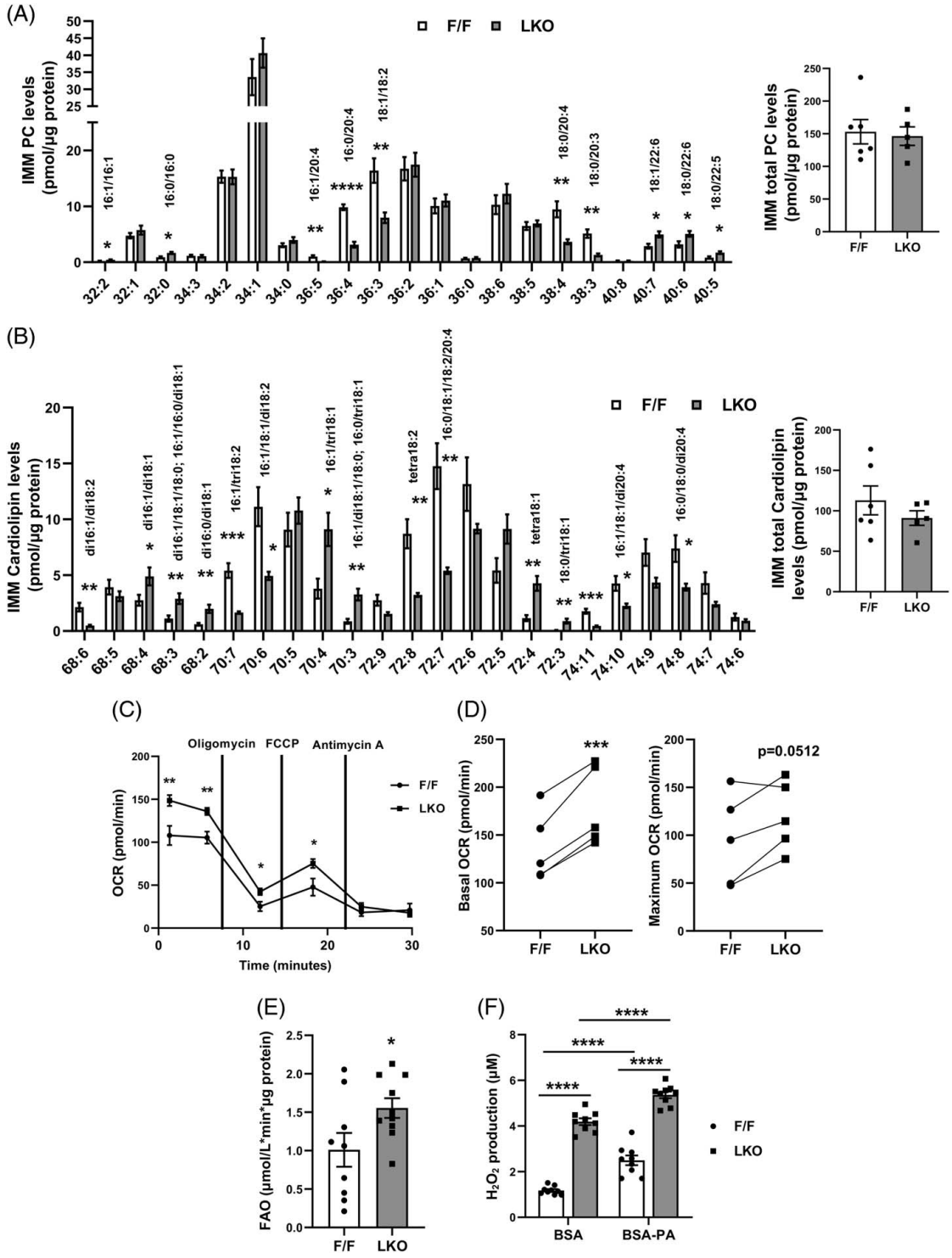

FIGURE 7 *Lpcat3* deficiency changes mitochondrial membrane composition and oxidative capacity. (A-B) Fatty acyl composition and total content of phosphatidylcholine (PC) (A) and cardiolipin (B) in inner mitochondrial membrane (IMM) in livers of F/F and LKO mice fed NASH diet for 12 weeks (n = 5~6/group). Indicated (*sn*-1/*sn*-2) molecular species were confirmed by product ion scanning for aliphatic composition. (C) Representative data of Seahorse mitochondrial stress test in isolated mitochondria from livers of F/F and LKO mice fed NASH diet for 12 weeks. (D) Basal and maximal oxygen consumption rates (OCRs) from Seahorse mitochondrial stress test of isolated mitochondria from livers of F/F and LKO mice on chow diet or NASH diet for 12 weeks. Paired data show repetitive experiments. (E) Fatty acid oxidation (FAO) rate of liver homogenate from F/F and LKO mice fed NASH diet for 12 weeks. (F) H_2O_2 production in primary hepatocytes isolated from chow diet-fed control and LKO mice with or without palmitate (250 µM) treatment. Data are presented as mean ± SEM. Statistical analysis was performed with multiple *t* test (A–C), paired *t* test (D and E), Student's t test (F), and 2-way ANOVA (G). *$p < 0.05$, **$p < 0.01$, ***$p < 0.001$, ****$p < 0.0001$. Abbreviations: IMM, inner mitochondrial membrane; LKO, Lpcat3 liver knockout mice; PC, phosphatidylcholine.

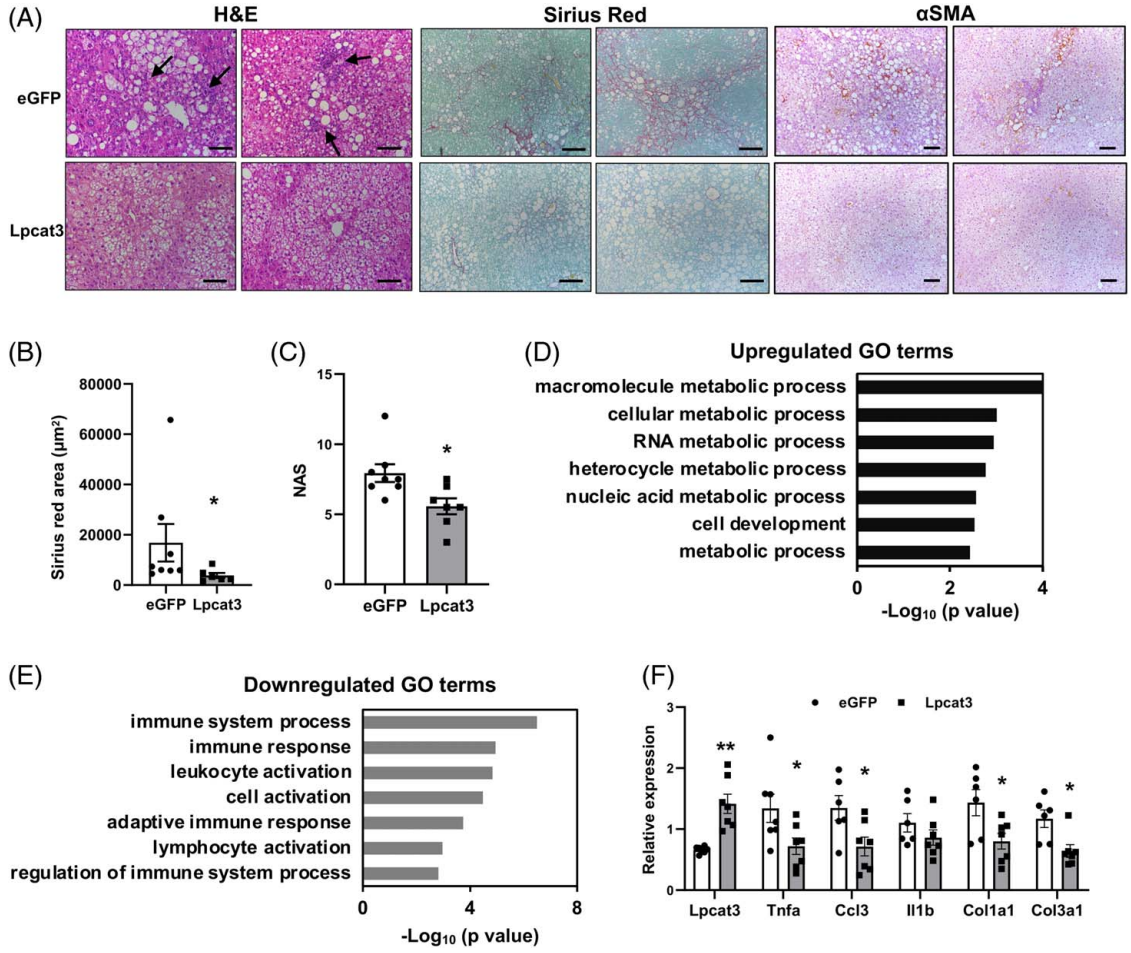

FIGURE 8 Overexpression of *Lpcat3* in the liver ameliorates diet-induced NASH progression. (A) H&E, Sirius Red, and immunohistochemistry of α-SMA of livers from *eGFP* and *Lpcat3* injected mice fed NASH diet. Arrows denote immune cell infiltration (scale bar, 100 μm). Quantifications of Sirius Red area (B) and NAS (C) of *eGFP* and *Lpcat3* injected mice fed NASH diet. (D, E) Enriched GO terms of significantly upregulated (D) and downregulated genes (E) in livers of *Lpcat3* injected mice compared with *eGFP*-injected mice based on RNA sequencing data. (F) Relative expression of *Lpcat3*, inflammation markers and collagen synthesis genes in livers of *eGFP* and *Lpcat3* injected mice fed NASH diet. Data are presented as mean ± SEM. Statistical analysis was performed with student's *t* test or multiple *t* test. $*p < 0.05$, $**p < 0.01$. Abbreviations: α-SMA, α-smooth muscle actin; GO, Gene Ontology.

was confirmed by immunoblotting with cellular compartment markers (Supplemental Figure S4C, http://links.lww.com/HEP/F18). The changes in mitochondrial complexes seemed to be a secondary effect of *Lpcat3* deficiency as their levels were not altered in *Lpcat3* acute knockdown cells (Supplemental Figure S4D, http://links.lww.com/HEP/F18). Electron microscopy (EM) analysis revealed altered mitochondrial morphology as demonstrated by more fragmented mitochondria in both chow diet-fed and NASH diet-fed LKO livers (Figure 5D). Quantification of mitochondrial morphology showed more circular mitochondria in LKO hepatocytes. Similar morphology change was also observed in *Lpcat3* knockdown cells stained with mitotracker (Supplemental Figure S4E, http://links.lww.com/HEP/F18). Interestingly, we also observed some mitochondria undergoing fission and autophagosome-like structures in the livers of LKO mice fed NASH diet (Figure 5D), suggesting that loss of *Lpcat3* may affect mitochondrial remodeling.

Lpcat3 deficiency alters mitochondrial dynamics and elevates stress-induced autophagy

We next investigated the mechanisms of decreased mitochondrial content and increased mitochondrial fragmentation in mice lacking *Lpcat3*. Mitochondrial homeostasis is regulated by a balance of mitochondrial biogenesis and degradation and mitochondrial fission/fusion.[29] There was no difference in the expression of *Pgc1a* and *Sirt1*, 2 genes involved in mitochondrial biogenesis, in NASH diet-fed mouse livers between genotypes (Supplemental Figure S5A, http://links.lww.com/HEP/F18), suggesting that reduced mitochondrial content is unlikely caused by altered mitochondrial biogenesis. Consistent with some mitochondria undergoing fission in EM analysis, we observed increased expression of DRP1 and reduced expression of OPA1 (Figure 6A), 2 proteins that play critical roles in fission and

fusion, respectively, indicating that loss of *Lpcat3* likely promotes mitochondrial fission but suppresses fusion, thereby resulting in more fragmented mitochondria.

Previous studies have demonstrated that ROS-mediated damages to the organelles induce autophagy as a responsive mechanism to clear damaged organelles.[30] It has been shown that 4-HNE–activated JNK pathway mediates the induction of autophagy response.[31] Considering that ROS/4-HNE production and JNK activation were enhanced in LKO livers, we hypothesized that loss of *Lpcat3* augments autophagy in response to increased oxidative stress and results in reduced mitochondria content. Indeed, we observed the presence of autophagosome structures in EM analysis of LKO liver sections (Figure 5D). To further test our hypothesis, we examined autophagy pathways in NASH diet-fed livers. Although there was no difference in early mitophagy markers, such as BNIP3, PINK1, or PARKIN levels, in both isolated mitochondria and whole liver lysate between control and LKO mice (Supplemental Figure S5B, C, http://links.lww.com/HEP/F18), markers of macroautophagy required for mitochondrial turnover by the lysosome, including ATG5-ATG12 conjugates and LC3 processing, were increased in LKO livers compared with controls (Figure 6B). It is well documented that lipid overload in hepatocytes, especially FFA and cholesterol, leads to organelle damage, inflammation, and fibrosis.[32,33] We next tested whether *Lpcat3* deficiency also potentiates autophagy response in the presence of lipid accumulation in primary hepatocytes. Consistent with *in vivo* results, FFA treatment increased LC3 processing in LKO hepatocytes (Supplemental Figure S5D, http://links.lww.com/HEP/F18). Interestingly, cholesterol treatment induced more pronounced autophagy response in LKO hepatocytes, including upregulation of ATG7, ATG5-ATG12 conjugate, and ATG16L1 (Supplemental Figure S5E, http://links.lww.com/HEP/F18). Furthermore, autophagy staining revealed more autophagic vacuoles in LKO hepatocytes compared with controls on starvation or cholesterol treatment (Figure 6C). Thus, ROS overproduction and lipid accumulation caused by *Lpcat3* deficiency likely work together to enhance autophagy in response to stress-induced damage in LKO livers.

Loss of *Lpcat3* increases IMM PL saturation and mitochondrial oxidation

Given that LPCAT3 functions through remodeling membrane PL, we hypothesized that *Lpcat3* deficiency may affect mitochondrial PL composition, thereby altering mitochondrial homeostasis. We focused on IMM because most of mitochondrial electron transport and oxidative phosphorylation occur in IMM. IMM was purified from mitochondria by osmotic swelling and ultracentrifugation. The enrichment of IMM was confirmed by western blot analysis of COX IV, an IMM localized protein (Supplemental Figure S6A, http://links.lww.com/HEP/F18). In agreement with LPCAT3 enzymatic activity, PL profiling showed dramatic decrease in polyunsaturated especially 18:2- and 20:4-containing PCs (Figure 7A, Supplemental Figure S6B, http://links.lww.com/HEP/F18 and Supplemental Table S1, http://links.lww.com/HEP/F17) and PEs (Supplemental Figure S6B, C, http://links.lww.com/HEP/F18) in the IMM of both chow-fed and NASH diet-fed LKO mice without affecting total PC or PE levels. Interestingly, the FA composition of cardiolipin (CL), another class of essential mitochondria-specific PLs, was also drastically altered in LKO livers as demonstrated by significant reduction in 18:2- and 20:4-containing CLs (Figure 7B, Supplemental Figure S6B, http://links.lww.com/HEP/F18 and Supplemental Table S2, http://links.lww.com/HEP/F17), whereas total CL levels were not changed. Mitochondrial membrane PL composition has been shown to be critical in modulating mitochondria functions, including oxidative respiration and ROS production.[34] Next, we evaluated the effect of *Lpcat3* deficiency on mitochondria function by seahorse analysis. Consistent with increased mitochondrial complexes, both basal and maximal oxygen consumption rates were higher in mitochondria isolated from NASH diet-fed LKO mice (Figure 7C-D), which was also confirmed in *Lpcat3* acute knockdown cells (Supplemental Figure S6C, http://links.lww.com/HEP/F18). Moreover, LKO mitochondria showed increased fatty acid oxidation compared with controls (Figure 7E), which is known to be a major source of ROS production.[35] Indeed, LKO hepatocytes produced ~3.5-fold and ~2.2-fold more H_2O_2 under basal and palmitate-treated conditions, respectively (Figure 7F). Thus, these data suggest that increasing IMM saturation by *Lpcat3* deficiency may enhance mitochondrial oxidative phosphorylation, which contributes to ROS overproduction and leads to cell damage, inflammation, and NASH progression.

Overexpression of *Lpcat3* in the liver ameliorates diet-induced NASH progression

Our results demonstrated that loss of *Lpcat3 per se* is sufficient to promote the initiation and progression of NASH in mice and that downregulation of *LPCAT3* is likely involved in the pathogenesis of NASH in at least some human patients. We next examined whether the overexpression of *Lpcat3* could attenuate steatosis to NASH progression. To test this, we fed C57BL/6 mice with NASH diet for 7 weeks to initiate steatosis, and then i.v. injected AAV encoding eGFP control or *Lpcat3* driven by a liver-specific TBG promoter, followed by another 9 weeks of diet feeding (Supplemental Figure S7A, http://links.lww.com/HEP/F18). There was no body weight difference between control and *Lpcat3* overexpression

mice during the diet feeding (Supplemental Figure S7B, http://links.lww.com/HEP/F18). Liver weight-to-body weight ratio was decreased by >20% in *Lpcat3*-overexpressing mice compared with eGFP-injected control mice (Supplemental Figure S7C, http://links.lww.com/HEP/F18). Lipid quantification showed slight decrease in hepatic TG and free cholesterol levels but not total cholesterol or NEFA levels in *Lpcat3*-overexpressing mice (Supplemental Figure S7D, http://links.lww.com/HEP/F18). Serum TG and cholesterol levels were also trended toward a decrease following *Lpcat3* overexpression (Supplemental Figure S7E, http://links.lww.com/HEP/F18). Histology analysis revealed less steatosis, inflammation, fibrosis, and activated HSCs in *Lpcat3*-overexpressing livers (Figure 8A, B). Accordingly, *Lpcat3* overexpression lowered NAS compared with eGFP controls (Figure 8C). Serum alanine transaminase and aspartate transaminase activities were also reduced by *Lpcat3* overexpression (Supplemental Figure S7F, http://links.lww.com/HEP/F18), suggesting less liver damage. RNA sequencing analysis revealed that metabolic processes were top GO terms among upregulated genes (Figure 8D), and the top processes among downregulated genes were all related to immune response or immune cell activation (Figure 8E), further corroborating that *Lpcat3* overexpression mitigates inflammation during NASH progression. Consistently, real-time RT-PCR analysis showed significant decrease in the expression of *Tnfα, Ccl3*, and collagen synthesis genes in *Lpcat3*-overexpressing livers (Figure 8F). Western blot analysis demonstrated reduced 4-HNE levels in *Lpcat3* overexpression livers (Supplemental Figure S7G, http://links.lww.com/HEP/F18), indicating that *Lpcat3* overexpression attenuates inflammation and fibrosis during NASH progression at least partially through alleviating oxidative stress.

DISCUSSION

The prevalence of NASH, a progressive inflammatory form of NAFLD, is dramatically increasing and has emerged as a significant contributor to the health burden of chronic liver diseases.[36] Approximately 25% of patients with NASH will progress to liver cirrhosis and in some cases to HCC.[37] Despite much effort, the molecular mechanisms that underlie the progression of NASH are not well understood. Our data demonstrated that mice lacking *Lpcat3* in the liver develop spontaneous histopathological manifestations of NASH, suggesting that changes in membrane PL composition *per se* are sufficient to drive the pathogenesis of NASH. More importantly, *LPCAT3* expression is progressively decreased in human NAFLD and NASH livers and is inversely correlated with NAS and fibrosis stage, suggesting that suppression of *LPCAT3* likely contributes to the development of NAFLD/NASH in humans. These studies highlight a novel mechanism by which membrane PL remodeling modulates the pathogenesis of NASH.

Our studies provide insight into the potential mechanisms how genetic variants contribute to the pathogenesis of NASH. The loss-of-function variant (I148M) in *PNPLA3* gene is associated with increased risk of NASH.[38] Interestingly, the levels of polyunsaturated PCs are reduced in homozygous I148M livers.[9] Similarly, carriers of *TM6SF2* E167K variant have decreased expression of TM6SF2 and increased risk of NAFLD and NASH.[39] Further studies found that hepatic synthesis of PCs from polyunsaturated fatty acids is impaired in E167K livers, resulting in deficiency in polyunsaturated PCs.[8] In contrast, a missense variant (A165T) in *MARC1* gene has been shown to be protective against liver cirrhosis[40] and is associated with decreased severity of NASH.[7] Lipidomics analysis revealed that carriers of A165T variant have higher hepatic polyunsaturated PCs compared with noncarriers.[7] Taken together, these studies demonstrate that hepatic polyunsaturated PC content is inversely correlated with the risk or severity of NASH in humans. Our data provide direct *in vivo* evidence to support that changes in PC composition contribute to NASH pathogenesis. It would be of interest to examine whether *LPCAT3* expression is altered in the livers of patients carrying these variants.

Interestingly, metabolism of other PLs, such as phosphatidylinositol (PI), have also been associated with NASH in human and mouse models. GWAS studies have identified variants near membrane-bound O-acyltransferase domain-containing 7 (*MBOAT7*) locus to be associated with fibrosis in NASH.[41] *MBOAT7* encodes a lysophosphatidylinositol acyltransferase enzyme that preferentially catalyzes synthesis of arachidonoyl-containing phosphatidylinositol species. Several studies have demonstrated that *Mboat7* deficiency promotes steatosis and fibrosis.[42,43] It has been shown that *Mboat7* inhibition enhances lipogenesis and promotes inflammation and fibrosis likely due to the accumulation of its substrate lysophosphatidylinositol or metabolites derived from arachidonic acid. In contrast, there was no difference in LPC or arachidonic acid metabolite prostaglandin E2 (PGE2) between LKO and control mice (data not shown). Thus, the mechanism by which *Lpcat3* deficiency promotes NASH progression is likely different from that of *Mboat7* suppression.

Accumulating evidence suggests that mitochondria play a key role in the pathophysiology of NASH.[44] Strikingly, we found that mtDNA content was significantly reduced in the livers of both chow diet-fed and NASH diet-fed LKO mice. Furthermore, mtDNA content is gradually decreased with the progression of NAFLD/NASH in both control and LKO livers, suggesting that decrease in mitochondria content likely contributes to disease progression. It has been shown that mitochondrial dysfunction induces the overproduction of ROS,

which oxidizes vital cellular components such as DNA, lipids, and proteins, thereby inducing cell death and liver damage, triggering inflammatory responses and fibrosis in NASH livers.[45] Indeed, we observed enhanced ROS levels and byproducts of oxidative stress in LKO livers. Interestingly, both basal and maximal oxygen consumption rates are increased in purified mitochondria from LKO livers. Therefore, lipid accumulation and augmented mitochondrial fatty acid β-oxidation likely lead to ROS overproduction in LKO livers, which in turn causes enhanced mitochondrial damage and autophagy, resulting in less mtDNA content. In addition, loss of *Lpcat3* also leads to mitochondrial fragmentation, likely caused by increased mitochondrial fission and decreased fusion. Mitochondrial fission and fusion are important mechanisms to maintain functional mitochondria in response to stresses.[46] Fusion helps alleviate stress by mixing the contents of partially damaged mitochondria, while fission removes damaged mitochondria and promotes apoptosis in the presence of high levels of cellular stress. Thus, altered mitochondrial dynamics in LKO livers could be a compensatory response induced by excessive stress and damage.

In agreement with LPCAT3 enzymatic activity, there is dramatic decrease in polyunsaturated PCs in the IMM, where electron transport and oxidative phosphorylation occur. CL is another class of mitochondria-specific PLs that are composed of 2 phosphatidic acid groups linked by a glycerol. Interestingly, the composition of polyunsaturated fatty acid in CL is also dramatically decreased in LKO livers. Changes in CL fatty acyl composition have been implicated in etiology of mitochondrial dysfunction and its associated pathophysiological conditions that are characterized by increased levels of oxidative stress, including NAFLD/NASH, diabetes, neurodegeneration, and ageing.[34] Furthermore, it has been shown that increased ROS production requires fragmentation of mitochondria.[47] We observed more fragmented mitochondria in LKO livers. The altered mitochondrial morphology in LKO livers is likely a direct consequence of decreased PL unsaturation as acute knockdown of *Lpcat3* in Hepa cells also results in less mitochondrial network, but we cannot rule out the contribution of enhanced oxidative stress in LKO livers. Nevertheless, these data indicate that LPCAT3 and PL remodeling are critical in maintaining mitochondria homeostasis. Although the mechanism of *Lpcat3* deficiency in NASH development is likely to be multifactorial, our data showed that altered mitochondrial dynamics and function play important roles in NASH progression in the absence of *Lpcat3*.

Currently, there are no FDA-approved drugs or effective therapeutics for NASH other than lifestyle intervention, which is only effective at early stage of NASH. The observation that overexpression of *Lpcat3* in the liver reduces hepatic TG levels and attenuates inflammation and fibrosis is inspiring. Although further studies are needed to understand how *Lpcat3* overexpression affects lipid metabolism and the progression of NASH, these studies provided a proof of concept that manipulating *LPCAT3* expression or activity could represent a novel therapeutic strategy for NASH.

AUTHOR CONTRIBUTIONS

Ye Tian designed and performed experiments, analyzed data, and wrote the paper. Kritika Mehta, Sun Mi Seok, Matthew J. Jellinek, Wei Lu, and Ruicheng Shi performed experiments and analyzed data. Shanny H. Kuo evaluated the histology. Gee W. Lau Jongsook K. Kemper, David A. Ford and Kai Zhang designed experiments and analyzed data. Richard Lee designed and synthesized antisense oligonucleotides. Bo Wang conceived the project, designed experiments, analyzed data, supervised the project, and wrote the paper.

ACKNOWLEDGMENTS

The authors thank Dr. Hui Xu at the Tumor Engineering and Phenotyping Shared Resources (TEP) of Cancer Center at Illinois for technical support with Seahorse analysis, Karen Doty at the Comparative Biosciences Histology Laboratory, and Figen A. Seiler at Electron Microscopy Core of University of Illinois at Chicago for technical support with histology analysis and electron microscopy analysis. RNA sequencing analysis was performed by high-throughput DNA sequencing core facility of Roy J. Carver Biotechnology Center (CBC) at University of Illinois at Urbana-Champaign. Metabolomics analysis was performed by the Metabolomics Core Facility at Robert H. Lurie Comprehensive Cancer Center of Northwestern University. Graphic abstract was created with BioRender.

FUNDING INFORMATION

This work was supported by grants from National Institute of Health (NIH) (DK114373 and DK128167 to Bo Wang, DK062777 and DK095842 to Jongsook K. Kemper, GM132438 to Kai Zhang, and Lipidomic core grant S10OD025246 to David A. Ford), Pfizer Global Medical Grant (70228131), start-up funds from the University of Illinois at Urbana-Champaign, seed grant and Tumor Engineering Phenotyping (TEP) shared resource utilization grant from Cancer Center at Illinois of UIUC, and Burnsides Laboratory Research Fund to Bo Wang.

CONFLICTS OF INTEREST

Richard Lee owns stock in and is employed by Verve Therapeutics. The remaining authors have no conflicts to report.

ORCID

Ye Tian https://orcid.org/0000–0002–7462–8082
Kritika Mehta https://orcid.org/0000–0002–4312–9950

Sun Mi Seok https://orcid.org/0009–0002–3805–7830
Shanny H. Kuo https://orcid.org/0000–0001–8924–6960
Wei Lu https://orcid.org/0000–0003–1310–9999
Ruicheng Shi https://orcid.org/0000–0001–9426–213X
Gee W. Lau https://orcid.org/0000–0002–7962–3950
Jongsook Kim Kemper https://orcid.org/0000–0002–5534–0286
Kai Zhang https://orcid.org/0000–0002–6687–4558
David A. Ford https://orcid.org/0000–0002–0029–1560
Bo Wang https://orcid.org/0000–0001–9234–035X

REFERENCES

1. Huang DQ, El-Serag HB, Loomba R. Global epidemiology of NAFLD-related HCC: trends, predictions, risk factors and prevention. Nat Rev Gastroenterol Hepatol. 2021;18:223–38.
2. Friedman SL, Neuschwander-Tetri BA, Rinella M, Sanyal AJ. Mechanisms of NAFLD development and therapeutic strategies. Nat Med. 2018;24:908–22.
3. Eslam M, Valenti L, Romeo S. Genetics and epigenetics of NAFLD and NASH: Clinical impact. J Hepatol. 2018;68:268–79.
4. Sookoian S, Pirola CJ, Valenti L, Davidson NO. Genetic pathways in nonalcoholic fatty liver disease: insights from systems biology. Hepatology. 2020;72:330–46.
5. Puri P, Baillie RA, Wiest MM, Mirshahi F, Choudhury J, Cheung O, et al. A lipidomic analysis of nonalcoholic fatty liver disease. Hepatology. 2007;46:1081–90.
6. Ooi GJ, Meikle PJ, Huynh K, Earnest A, Roberts SK, Kemp W, et al. Hepatic lipidomic remodeling in severe obesity manifests with steatosis and does not evolve with non-alcoholic steatohepatitis. J Hepatol. 2021;75:524–35.
7. Luukkonen PK, Juuti A, Sammalkorpi H, Penttila AK, Oresic M, Hyotylainen T, et al. MARC1 variant rs2642438 increases hepatic phosphatidylcholines and decreases severity of non-alcoholic fatty liver disease in humans. J Hepatol. 2020;73:725–6.
8. Luukkonen PK, Zhou Y, Nidhina Haridas PA, Dwivedi OP, Hyotylainen T, Ali A, et al. Impaired hepatic lipid synthesis from polyunsaturated fatty acids in TM6SF2 E167K variant carriers with NAFLD. J Hepatol. 2017;67:128–36.
9. Luukkonen PK, Nick A, Holtta-Vuori M, Thiele C, Isokuortti E, Lallukka-Bruck S, et al. Human PNPLA3-I148M variant increases hepatic retention of polyunsaturated fatty acids. JCI Insight. 2019;4:e127902.
10. Lands WE. Metabolism of glycerolipides; a comparison of lecithin and triglyceride synthesis. J Biol Chem. 1958;231:883–8.
11. Wang B, Tontonoz P. Phospholipid remodeling in physiology and disease. Annu Rev Physiol. 2019;81:165–88.
12. Rong X, Wang B, Dunham MM, Hedde PN, Wong JS, Gratton E, et al. Lpcat3-dependent production of arachidonoyl phospholipids is a key determinant of triglyceride secretion. Elife. 2015;4:e06557.
13. Kim YC, Seok S, Zhang Y, Ma J, Kong B, Guo G, et al. Intestinal FGF15/19 physiologically represses hepatic lipogenesis in the late fed-state by activating SHP and DNMT3A. Nat Commun. 2020;11:5969.
14. Fujiwara N, Kubota N, Crouchet E, Koneru B, Marquez CA, Jajoriya AK, et al. Molecular signatures of long-term hepatocellular carcinoma risk in nonalcoholic fatty liver disease. Sci Transl Med. 2022;14:eabo4474.
15. Rong X, Wang B, Palladino EN, de Aguiar Vallim TQ, Ford DA, Tontonoz P. ER phospholipid composition modulates lipogenesis during feeding and in obesity. J Clin Invest. 2017;127:3640–51.
16. Wang B, Rong X, Duerr MA, Hermanson DJ, Hedde PN, Wong JS, et al. Intestinal phospholipid remodeling is required for dietary-lipid uptake and survival on a high-fat diet. Cell Metab. 2016;23:492–504.
17. Wang B, Rong X, Palladino END, Wang J, Fogelman AM, Martin MG, et al. Phospholipid remodeling and cholesterol availability regulate intestinal stemness and tumorigenesis. Cell Stem Cell. 2018;22:206– e204.
18. Bligh EG, Dyer WJ. A rapid method of total lipid extraction and purification. Can J Biochem Physiol. 1959;37:911–7.
19. Amunugama K, Jellinek MJ, Kilroy MP, Albert CJ, Rasi V, Hoft DF, et al. Identification of novel neutrophil very long chain plasmalogen molecular species and their myeloperoxidase mediated oxidation products in human sepsis. Redox Biol. 2021;48:102208.
20. Tsuchida T, Lee YA, Fujiwara N, Ybanez M, Allen B, Martins S, et al. A simple diet- and chemical-induced murine NASH model with rapid progression of steatohepatitis, fibrosis and liver cancer. J Hepatol. 2018;69:385–95.
21. Rong X, Albert CJ, Hong C, Duerr MA, Chamberlain BT, Tarling EJ, et al. LXRs regulate ER stress and inflammation through dynamic modulation of membrane phospholipid composition. Cell Metab. 2013;18:685–97.
22. Zhang XQ, Xu CF, Yu CH, Chen WX, Li YM. Role of endoplasmic reticulum stress in the pathogenesis of nonalcoholic fatty liver disease. World J Gastroenterol. 2014;20:1768–76.
23. Zorov DB, Juhaszova M, Sollott SJ. Mitochondrial reactive oxygen species (ROS) and ROS-induced ROS release. Physiol Rev. 2014;94:909–50.
24. Lykkesfeldt J. Ascorbate and dehydroascorbic acid as reliable biomarkers of oxidative stress: analytical reproducibility and long-term stability of plasma samples subjected to acidic deproteinization. Cancer Epidemiol Biomarkers Prev. 2007;16:2513–6.
25. Garcia-Ruiz C, Fernandez-Checa JC. Mitochondrial oxidative stress and antioxidants balance in fatty liver disease. Hepatol Commun. 2018;2:1425–39.
26. Win S, Than TA, Zhang J, Oo C, Min RWM, Kaplowitz N. New insights into the role and mechanism of c-Jun-N-terminal kinase signaling in the pathobiology of liver diseases. Hepatology. 2018;67:2013–4.
27. Li S, Tan HY, Wang N, Zhang ZJ, Lao L, Wong CW, et al. The role of oxidative stress and antioxidants in liver diseases. Int J Mol Sci. 2015;16:26087–124.
28. Peng KY, Watt MJ, Rensen S, Greve JW, Huynh K, Jayawardana KS, et al. Mitochondrial dysfunction-related lipid changes occur in nonalcoholic fatty liver disease progression. J Lipid Res. 2018;59:1977–86.
29. Detmer SA, Chan DC. Functions and dysfunctions of mitochondrial dynamics. Nat Rev Mol Cell Biol. 2007;8:870–9.
30. Filomeni G, De Zio D, Cecconi F. Oxidative stress and autophagy: the clash between damage and metabolic needs. Cell Death Differ. 2015;22:377–88.
31. Haberzettl P, Hill BG. Oxidized lipids activate autophagy in a JNK-dependent manner by stimulating the endoplasmic reticulum stress response. Redox Biol. 2013;1:56–64.
32. Neuschwander-Tetri BA. Hepatic lipotoxicity and the pathogenesis of nonalcoholic steatohepatitis: the central role of nontriglyceride fatty acid metabolites. Hepatology. 2010;52:774–88.
33. Ioannou GN. The role of cholesterol in the pathogenesis of NASH. Trends Endocrinol Metab. 2016;27:84–95.
34. Shi Y. Emerging roles of cardiolipin remodeling in mitochondrial dysfunction associated with diabetes, obesity, and cardiovascular diseases. J Biomed Res. 2010;24:6–15.
35. Seifert EL, Estey C, Xuan JY, Harper ME. Electron transport chain-dependent and -independent mechanisms of mitochondrial H2O2 emission during long-chain fatty acid oxidation. J Biol Chem. 2010;285:5748–8.

36. Younossi Z, Anstee QM, Marietti M, Hardy T, Henry L, Eslam M, et al. Global burden of NAFLD and NASH: trends, predictions, risk factors and prevention. Nat Rev Gastroenterol Hepatol. 2018;15:11–20.
37. McCullough AJ. The clinical features, diagnosis and natural history of nonalcoholic fatty liver disease. Clin Liver Dis. 2004;8:521–33; viii.
38. Sookoian S, Pirola CJ. Meta-analysis of the influence of I148M variant of patatin-like phospholipase domain containing 3 gene (PNPLA3) on the susceptibility and histological severity of nonalcoholic fatty liver disease. Hepatology. 2011;53:1883–94.
39. Kozlitina J, Smagris E, Stender S, Nordestgaard BG, Zhou HH, Tybjaerg-Hansen A, et al. Exome-wide association study identifies a TM6SF2 variant that confers susceptibility to nonalcoholic fatty liver disease. Nat Genet. 2014;46:352–6.
40. Emdin CA, Haas ME, Khera AV, Aragam K, Chaffin M, Klarin D, et al. A missense variant in Mitochondrial Amidoxime Reducing Component 1 gene and protection against liver disease. PLoS Genet. 2020;16:e1008629.
41. Mancina RM, Dongiovanni P, Petta S, Pingitore P, Meroni M, Rametta R, et al. The MBOAT7-TMC4 variant rs641738 increases risk of nonalcoholic fatty liver disease in individuals of European Descent. Gastroenterology. 2016;150:1219–30 e1216.
42. Helsley RN, Varadharajan V, Brown AL, Gromovsky AD, Schugar RC, Ramachandiran I, et al. Obesity-linked suppression of membrane-bound O-acyltransferase 7 (MBOAT7) drives non-alcoholic fatty liver disease. Elife. 2019;8:e49882.
43. Xia M, Chandrasekaran P, Rong S, Fu X, Mitsche MA. Hepatic deletion of Mboat7 (LPIAT1) causes activation of SREBP-1c and fatty liver. J Lipid Res. 2021;62:100031.
44. Pessayre D, Fromenty B. NASH: a mitochondrial disease. J Hepatol. 2005;42:928–40.
45. George J, Pera N, Phung N, Leclercq I, Yun Hou J, Farrell G. Lipid peroxidation, stellate cell activation and hepatic fibrogenesis in a rat model of chronic steatohepatitis. J Hepatol. 2003;39:756–64.
46. Youle RJ, van der Bliek AM. Mitochondrial fission, fusion, and stress. Science. 2012;337:1062–5.
47. Yu T, Robotham JL, Yoon Y. Increased production of reactive oxygen species in hyperglycemic conditions requires dynamic change of mitochondrial morphology. Proc Natl Acad Sci USA. 2006;103:2653–8.

How to cite this article: Tian Y, Jellinek MJ, Mehta K, Seok SM, Kuo SH, Lu W, et al. Membrane phospholipid remodeling modulates nonalcoholic steatohepatitis progression by regulating mitochondrial homeostasis. Hepatology. 2024;79:882–897. https://doi.org/10.1097/HEP.0000000000000375